

Structures and interactions between two colloidal particles in adsorptive polymer solutions

Wenwu Li^a, Xingkun Man^a, Dong Qiu^a, Xinghua Zhang^b, Dadong Yan^{b,*}

^a Beijing National Laboratory for Molecular Sciences (BNLMS), Institute of Chemistry, Chinese Academy of Sciences, Beijing 100190, China

^b Department of Physics, Beijing Normal University, Beijing 100875, China

ARTICLE INFO

Article history:

Received 21 October 2011

Received in revised form

8 May 2012

Accepted 9 May 2012

Available online 17 May 2012

Keywords:

Adsorption

Bridge structure

Self-consistent field theory (SCFT)

ABSTRACT

The role of weak adsorptive polymer chains in the colloidal particles solution is studied by self-consistent field theory (SCFT). The numerical results show the potential between colloids are attractive interaction. Besides the depletion effects the chain conformations such as loop, tail and bridge between two spherical colloidal particles play important roles. The quantitative polymer concentration dependent chain conformations and then the effective potential are also addressed.

© 2012 Elsevier Ltd. All rights reserved.

1. Introduction

Two phenomena are very important in polymer physics study which are adsorption and depletion. Adsorption effect of colloid-polymer mixtures is widely studied in industrial and biological applications [1,2], such as adhesion, lubrication, improvement of the rheological and mechanical properties of a system, and so on. The adsorption is quite common in colloid-polymer mixtures. Usually, the polymer systems demonstrate distinctive phenomena due to the rich chain conformation. The conformation of an adsorbed polymer chain can be described in terms of loops and tails [3]. Moreover, if the chain is long enough, there exists another structure, bridge, which links different colloidal particles. In Ref. [4], the authors studied the loop and tail structures of adsorptive polymers on a single colloidal particle.

On the other hand, the depletion effect, also plays an important role in applications, such as wastewater treatment and protein crystallization. It is the result of the conformational entropy driving of polymer chains [5]. The depletion effect has been investigated extensively, as for two-plate [3,6–10]. However, the case of two sphere is very different, and less intensive than the two-plate case [5].

In the recent years, more and more people paid close attention to the studies of the so-called polymer-grafted particles, and many

theoretical methods are presented, such as scaling, the description of a colloidal particle clothed with polymers [11], and the interaction between polymer-grafted particles [12]. In these studies, the number of the polymer chains of the grafting surface, which describes by grafting density, is fixed. The chains can move on the grafting surface freely, but cannot escape from the surface. This corresponds to a strong-adsorptive case. In the present study, we focus on the system in which the polymers are fillers and physically are adsorbed on the colloids by using SCFT which is commonly used in polymer system [13–15].

In certain situations, it is interesting to investigate other structures, such as bridge, besides loop and tail. In Ref. [16], bridging and looping were studied in multiblock copolymer melts. The loop is defined by the configurations of which both ends of the block reside on the same interface, while the bridging is defined by the configurations of which connects one interface with another. At the same time, the author defined the fraction of the bridging. However, it is hard to generalize to other cases. In this paper, we investigate the structures mentioned above by dividing the propagator. There is of course another structure, namely, train structure. However, this structure will not be considered in the present case, since its physical effects are not important. We focus on the distributions of these three structures by employing SCFT in bispherical coordinate systems. The adsorption makes the colloidal particle clothed with polymers. But the number of polymers which cloth the colloidal particle is not fixed, it varies with the changes of the spacing of the two colloidal particles and some form the bridges, which is different from that in Ref. [12]. At the same time,

* Corresponding author.

E-mail addresses: dqiu@iccas.ac.cn (D. Qiu), yandd@bnu.edu.cn (D. Yan).

we investigate the potential between the two spheres. It is different from that in Ref. [5], which is nonadsorptive polymer solution, and also different from that in Ref. [4], which is strong-adsorptive and in a single spherical coordinate system. Thus the present case can fill the gap between Ref. [5] and Ref. [12].

This paper is organized as follows. In Section 2, we outline the SCFT for a polymer solution in the grand canonical ensemble, and describe the three kinds of structures. Also we develop the numerical method to solve the self-consistent field equations in the bispherical coordinate. In Section 3, we give the results and discussions. In Section 4, we present the conclusions.

2. Theory and numerical methods

2.1. Theory

In this paper, we consider an adsorptive polymer solution with colloidal particles, which have the same radius, R . The statistical segment length b , and the factor of $k_B T$ are taken as the units of length and energy, respectively. For an incompressible polymer solution in volume of V , its grand potential in equilibrium with a bulk reservoir is given by [20,21].

$$\frac{G}{k_B T} = \int_V d\mathbf{r} [\chi \phi_p(\mathbf{r}) \phi_s(\mathbf{r}) - \omega_p(\mathbf{r}) \phi_p(\mathbf{r}) - \omega_s(\mathbf{r}) \phi_s(\mathbf{r})] - e^{\Delta\mu_p} Q_p - e^{\Delta\mu_s} Q_s, \quad (1)$$

where χ is the Flory–Huggins parameter, which characterizes the effective interaction between solvent molecules and polymer segments; $\phi_j(\mathbf{r})$ is the volume fraction, and $\sum_j \phi_j(\mathbf{r}) = 1$; $\omega_j(\mathbf{r})$ is the corresponding self-consistent field; $\Delta\mu_j$ is the exchange chemical potential, where all the above $j = p$ for polymer or s for solvent; Q_s is the partition function for the solvent molecule in the field of $\omega_s(\mathbf{r})$, given by $Q_s = \int d\mathbf{r} e^{-\omega_s(\mathbf{r})}$; Q_p is the single chain partition function in field of $\omega_p(\mathbf{r})$, given by $Q_p = \int d\mathbf{r} q_p(\mathbf{r}, N)$, where $q_p(\mathbf{r}, N)$ is the propagator of the chain with the degree of polymerization N and one end at the spatial position \mathbf{r} . Propagator $q_p(\mathbf{r}, N)$ is determined by the modified diffusion equation.

$$\frac{\partial}{\partial t} q_p(\mathbf{r}, t) = \frac{b^2}{6} \nabla^2 q_p(\mathbf{r}, t) - \omega_p(\mathbf{r}) q_p(\mathbf{r}, t), \quad (2)$$

where t is the arc length along polymer chain. In the following discussions, we omit the subscript “ p ” for convenience. The initial condition is $q(\mathbf{r}, 0) = 1$. As the boundary condition, there is a boundary condition $\partial q / \partial x + \kappa q = 0$ at $x = 0$ suggested by de Gennes in his famous book [7], and this is a 1-dimensional equation. In our case, it is difficult to define a similar adsorbed layer profile such as in Ref. [4], because the bispherical coordinate is a non-uniform mesh. Considering the calculability for our cases, we use the boundary condition, $\nabla q(\mathbf{r}, t) \cdot \hat{\mathbf{n}} + \kappa q(\mathbf{r}, t) = 0$, instead of defining an adsorbed layer profile [4], where the unit vector $\hat{\mathbf{n}}$ is the exterior normal vector of the spherical surface, while κ is the parameter which characterizes the adsorptive interaction. This is a 3-dimensional equation which is similar to the 1-dimensional case. According to de Gennes, when $\kappa \cdot \xi \ll 1$, it is called weakly adsorbed [7], where ξ is the range of interaction, which is assumed to be small of order of Kuhn length. By the way, as in many studies, the interaction between two colloidal particles is ignored in our study. Moreover, $q(\mathbf{r}, t)$ equals the value of the bulk phase at infinity.

The density profiles $\phi_p(\mathbf{r})$ and $\phi_s(\mathbf{r})$ and the corresponding auxiliary fields $\omega_p(\mathbf{r})$ and $\omega_s(\mathbf{r})$ can be obtained from the following self-consistent field equations:

$$\omega_p(\mathbf{r}) - \omega_s(\mathbf{r}) = \chi [1 - 2\phi_p(\mathbf{r})], \quad (3)$$

$$\phi_p(\mathbf{r}) = e^{\Delta\mu_p} \int_0^N dt q_p(\mathbf{r}, t) q_p(\mathbf{r}, N - t), \quad (4)$$

$$\phi_s(\mathbf{r}) = e^{\Delta\mu_s} e^{-\omega_s(\mathbf{r})}. \quad (5)$$

The choices of $\Delta\mu_p$ and $\Delta\mu_s$ are the same as in Ref. [5].

After obtaining the density profiles and the self-consistent fields, we calculate the excess free energy with respect to the homogenous state,

$$\Delta F(d) = G(d) - G_0, \quad (6)$$

where $d = D - 2R$, which is the separation between the surfaces along the line of centers of two spheres with radius R and center–center distance D ; G_0 is the grand potential of bulk phase in V given in Ref. [5].

The potential $U(d)$ between the two spheres is given by,

$$U(d) = \Delta F(d) - \Delta F(\infty). \quad (7)$$

2.2. Sketch of the bispherical coordinate systems

It is appropriate to adopt the bispherical coordinate system for the present case. So let us recall it briefly at first, the reader who interests in it can find the detailed description in Refs. [17–19].

The relations between bispherical coordinates (η, θ, φ) and Cartesian coordinates (x, y, z) are given by,

$$x = \frac{a \sin \theta \cos \varphi}{\cosh \eta - \cos \theta}, \quad y = \frac{a \sin \theta \sin \varphi}{\cosh \eta - \cos \theta}, \quad z = \frac{a \sinh \eta}{\cosh \eta - \cos \theta}, \quad (8)$$

where a is the distance from the origin, which is defined by $\eta = 0$ and $\theta = \pi$, to the poles, of which $\eta = \pm \infty$. In this paper, we take η_+ and η_- as the η coordinates of the spherical surfaces. We have $\eta_+ = (1/2) \ln [(\beta^2 - 2)/2 + \beta^4 - 4\beta^2/2]$, and obviously $\eta_- = -\eta_+$, where $\beta = D/R$. Henceforth, we call one sphere as η_+ and another as η_- . The constant- θ surfaces are perpendicular to the constant- η surfaces.

Using the transformation of the integral measures in different coordinate systems, we obtain the metric coefficients associated with the bispherical coordinates $h_\eta = h_\theta = a/Q(\eta, \theta)$ and $h_\varphi = a \sin \theta / Q(\eta, \theta)$, where $Q(\eta, \theta) = \cosh \eta - \cos \theta$. In the discussions, φ will be omitted because of the symmetry. We use a uniform mesh to discrete the (η, θ) space as follows,

$$\eta_i = \frac{i}{N_\eta} \eta_+, \quad i = -N_\eta, \dots, N_\eta; \quad (9)$$

$$\theta_j = \frac{j\pi}{N_\theta}, \quad j = 0, 1, \dots, N_\theta. \quad (10)$$

The point (0,0) represents the infinity.

2.3. Theory continued

To study the distributions of different conformation structures of the polymer chains, we divide the propagator $q(\mathbf{r}, t)$ into four parts,

$$q(\mathbf{r}, t) = q^{a+}(\mathbf{r}, t) + q^{a-}(\mathbf{r}, t) + q^f(\mathbf{r}, t) + q^{a\pm}(\mathbf{r}, t), \quad (11)$$

where $q^{a+}(\mathbf{r},t)$ and $q^{a-}(\mathbf{r},t)$ denote the propagators which adsorb on the constant- η surfaces of η_+ and η_- , respectively; $q^f(\mathbf{r},t)$ is the free part, namely adsorbs neither on η_+ nor on η_- ; $q^{a\pm}(\mathbf{r},t)$ denotes the propagator which adsorbs both on η_+ and on η_- . With these four propagators, we define the distributions of volume fraction of segments in the spatial point \mathbf{r} which coming from free, loop, tail, bridge chains, respectively, given by,

$$\phi^{\text{free}}(\mathbf{r}) = e^{\Delta\mu_p} \int dt q^f(\mathbf{r},t)q^f(\mathbf{r},N-t), \quad (12)$$

$$\phi^{\text{loop}}(\mathbf{r}) = e^{\Delta\mu_p} \int dt [q^{a+}(\mathbf{r},t)q^{a+}(\mathbf{r},N-t) + q^{a-}(\mathbf{r},t)q^{a-}(\mathbf{r},N-t)], \quad (13)$$

$$\phi^{\text{tail}}(\mathbf{r}) = 2e^{\Delta\mu_p} \int dt q^f(\mathbf{r},t) [q^{a+}(\mathbf{r},N-t) + q^{a-}(\mathbf{r},N-t) + q^{a\pm}(\mathbf{r},N-t)], \quad (14)$$

$$\phi^{\text{bridge}}(\mathbf{r}) = 1 - \phi^{\text{free}}(\mathbf{r}) - \phi^{\text{loop}}(\mathbf{r}) - \phi^{\text{tail}}(\mathbf{r}). \quad (15)$$

By the way, when we talking about the distribution of volume fraction of segments, we fix the spatial point \mathbf{r} . In other words, we consider the contribution belongs to which configuration in the fixed spatial point \mathbf{r} .

Furthermore, we can obtain the average tail length l_{tail} in bispherical coordinates. For η_+ sphere, it is given by,

$$l_{\text{tail}}^{\eta_+}(\theta) = \lim_{\eta \rightarrow \eta_+} \frac{\int tq^f(\eta,\theta,t)q^a(\eta,\theta,N-t)dt}{\int q^f(\eta,\theta,t)q^a(\eta,\theta,N-t)dt}. \quad (16)$$

Obviously, the average tail length of η_- sphere is the same as that of η_+ for symmetry.

2.4. Further discussions of the initial and boundary conditions

In the bispherical coordinate system, the propagator can be rewritten as follows,

$$q(\eta,\theta;t) = q^{a+}(\eta,\theta;t) + q^{a-}(\eta,\theta;t) + q^f(\eta,\theta;t) + q^{a\pm}(\eta,\theta;t), \quad (17)$$

where $q(\eta,\theta;t)$ is the total propagator, which satisfies the initial condition $q(\eta,\theta;0) = 1$, and the boundary conditions,

$$[\nabla q(\eta,\theta;t) \cdot \hat{\mathbf{n}} + \kappa q(\eta,\theta;t)]|_{\eta=\eta_+,\eta_-} = 0, \quad (18)$$

$$\frac{\partial}{\partial\theta}q(\eta,\theta;t)\Big|_{\theta=0,\pi} = 0. \quad (19)$$

Here, the meanings of $\hat{\mathbf{n}}$ and κ can be found in the above discussions, and the detailed derivation of above boundary conditions in bispherical coordinates is provided in the Appendix. The propagator $q^{a+}(\eta,\theta;t)$ denotes the propagator which adsorbs on η_+ , which satisfies the initial condition $q^{a+}(\eta,\theta;0) = 1$, and the boundary conditions,

$$[\nabla q^{a+}(\eta,\theta;t) \cdot \hat{\mathbf{n}} + \kappa q^{a+}(\eta,\theta;t)]\Big|_{\eta=\eta_+} = -\nabla q^f(\eta,\theta;t) \cdot \hat{\mathbf{n}}\Big|_{\eta=\eta_+}, \quad (20)$$

$$\frac{\partial}{\partial\theta}q^{a+}(\eta,\theta;t)\Big|_{\theta=0,\pi} = 0, \quad (21)$$

$$q^{a+}(\eta,\theta;t)\Big|_{\eta=\eta_-} = 0. \quad (22)$$

Similarly, we have the definition for the propagator $q^{a-}(\eta,\theta;t)$ if we use η_- instead of η_+ in the above three equations. The propagator $q^f(\eta,\theta;t)$ is the free part with the initial condition $q^f(\eta,\theta;0) = 1$, and the boundary condition

$$q^f(\eta,\theta;t)\Big|_{\eta=\eta_+,\eta_-} = 0. \quad (23)$$

The propagator $q^{a\pm}(\eta,\theta;t)$ can be obtained by the above other four propagators.

2.5. Numerical methods for solving the modified diffusion equation

Now we employ the finite difference method and alternating direction implicit (ADI) method to solve the modified diffusion equation. The modified diffusion equation in the bispherical system is given by [5,19],

$$\begin{aligned} \frac{\partial q(\eta,\theta;t)}{\partial t} = & \frac{b^2 Q^2}{6 a^2} \left[\frac{\partial^2}{\partial\eta^2}q(\eta,\theta;t) - \frac{\sinh \eta}{Q} \frac{\partial}{\partial\eta}q(\eta,\theta;t) \right. \\ & \left. + \frac{\partial^2}{\partial\theta^2}q(\eta,\theta;t) + \frac{1 \cosh \eta \cos \theta - 1}{Q \sin \theta} \frac{\partial}{\partial\theta}q(\eta,\theta;t) \right] \\ & - \omega(\eta,\theta)q(\eta,\theta;t). \end{aligned} \quad (24)$$

The initial condition of propagator $q(\eta,\theta;t)$ is $q(\eta,\theta;0) = 1$ for all (η,θ) , but the boundary conditions here are different from those in Ref. [5]. Instead, we use $\nabla q(\eta,\theta;t) \cdot \hat{\mathbf{n}} + \kappa q(\eta,\theta;t) = 0$ for $\eta = \eta_+$ or $\eta = \eta_-$, and $\partial q(\eta,\theta;t)/\partial\theta = 0$ for $\theta = 0$ or $\theta = \pi$. However, when we take $\theta \rightarrow 0$ and $\theta \rightarrow \pi$, we must be careful, for,

$$\lim_{\theta \rightarrow 0,\pi} \frac{\cosh \eta \cos \theta - 1}{Q \sin \theta} \frac{\partial}{\partial\theta}q(\eta,\theta;t) = \frac{\partial^2}{\partial\theta^2}q(\eta,\theta;t), \quad (25)$$

which makes the modified diffusion equation to reduce to those in Ref. [5,19],

$$\begin{aligned} \frac{\partial q(\eta,\theta;t)}{\partial t} = & \frac{b^2 Q^2}{6 a^2} \left[\frac{\partial^2}{\partial\eta^2}q(\eta,\theta;t) - \frac{\sinh \eta}{Q} \frac{\partial}{\partial\eta}q(\eta,\theta;t) \right. \\ & \left. + 2 \frac{\partial^2}{\partial\theta^2}q(\eta,\theta;t) \right] - \omega(\eta,\theta)q(\eta,\theta;t). \end{aligned} \quad (26)$$

The steps of discretizing the modified diffusion equation in the uniform mesh of the space (η,θ) using the finite difference method are the same as those in Ref. [5], and the derivatives of any function $f(\eta,\theta)$ at point (η_i,θ_j) are replaced by,

$$\frac{\partial}{\partial\eta}f_{i,j} = \frac{f_{i+1,j} - f_{i-1,j}}{2\Delta\eta}, \quad (27)$$

$$\frac{\partial}{\partial\theta}f_{i,j} = \frac{f_{i,j+1} - f_{i,j-1}}{2\Delta\theta}, \quad (28)$$

$$\frac{\partial^2}{\partial\eta^2}f_{i,j} = \frac{f_{i+1,j} + f_{i-1,j} - 2f_{i,j}}{(\Delta\eta)^2}, \quad (29)$$

$$\frac{\partial^2 f_{ij}}{\partial \theta^2} = \frac{f_{i,j+1} + f_{i,j-1} - 2f_{ij}}{(\Delta\theta)^2}, \quad (30)$$

where $\Delta\eta$ and $\Delta\theta$ are the step sizes of the uniform mesh, $\Delta\eta = \eta_+ / N_\eta$, and $\Delta\theta = \pi / N_\theta$. Thus we obtain the discretized modified diffusion equation,

$$\begin{aligned} \frac{\partial}{\partial t} q_{ij} = & \frac{b^2 Q_{ij}^2}{6 a^2} \left[\frac{q_{i+1,j} + q_{i-1,j} - 2q_{ij}}{(\Delta\eta)^2} - \frac{\sinh \eta_i q_{i+1,j} - q_{i-1,j}}{Q_{ij} 2\Delta\eta} \right. \\ & \left. + \frac{1}{Q_{ij}} \frac{\cosh \eta_i \cos \theta_j - 1}{\sin \theta_j} \frac{q_{i,j+1} - q_{i,j-1}}{2\Delta\theta} + \frac{q_{i,j+1} + q_{i,j-1} - 2q_{ij}}{(\Delta\theta)^2} \right] \\ & - \omega_{ij} q_{ij}. \end{aligned} \quad (31)$$

The cases $\theta = 0$ and π are the same as the above treatments.

We discretized the so-called “time” variable t as $t = k\Delta t$, where $k = 0, 1, \dots, N_t$, $\Delta t = N/N_t$ is the “time” step. All above discretized equations can be solved by the method of solving band diagonal equations implicitly along alternating directions [22] within the framework of ADI method. In order to obtain the propagator q_{ij}^{k+1} at next “time”, $(k+1)\Delta t$, from the propagator q_{ij}^k at any initial “time”, $k\Delta t$, we introduce the function q_{ij}^* at the middle “time”, $k\Delta t/2$. Firstly, we calculate q_{ij}^* from q_{ij}^k in the η -direction, given by

$$\begin{aligned} \frac{q_{ij}^* - q_{ij}^k}{\Delta t/2} = & \frac{b^2 Q_{ij}^2}{6 a^2} \left[\frac{q_{i+1,j}^* + q_{i-1,j}^* - 2q_{ij}^*}{(\Delta\eta)^2} - \frac{\sinh \eta_i q_{i+1,j}^* - q_{i-1,j}^*}{Q_{ij} 2\Delta\eta} \right. \\ & \left. + \frac{1}{Q_{ij}} \frac{\cosh \eta_i \cos \theta_j - 1}{\sin \theta_j} \frac{q_{i,j+1}^k - q_{i,j-1}^k}{2\Delta\theta} \right. \\ & \left. + \frac{q_{i,j+1}^k + q_{i,j-1}^k - 2q_{ij}^k}{(\Delta\theta)^2} \right] - \omega_{ij} q_{ij}^k. \end{aligned} \quad (32)$$

For each j line we can obtain q_{ij}^* by solving the tridiagonal equation from the above equation with the corresponding boundary conditions. After obtaining q_{ij}^* , we can obtain the propagator q_{ij}^{k+1} in the θ -direction as follows,

$$\begin{aligned} \frac{q_{ij}^{k+1} - q_{ij}^*}{\Delta t/2} = & \frac{b^2 Q_{ij}^2}{6 a^2} \left[\frac{q_{i+1,j}^{k+1} + q_{i-1,j}^{k+1} - 2q_{ij}^{k+1}}{(\Delta\eta)^2} \right. \\ & \left. - \frac{\sinh \eta_i q_{i+1,j}^{k+1} - q_{i-1,j}^{k+1}}{Q_{ij} 2\Delta\eta} \right. \\ & \left. + \frac{1}{Q_{ij}} \frac{\cosh \eta_i \cos \theta_j - 1}{\sin \theta_j} \frac{q_{i,j+1}^* - q_{i,j-1}^*}{2\Delta\theta} \right. \\ & \left. + \frac{q_{i,j+1}^* + q_{i,j-1}^* - 2q_{ij}^*}{(\Delta\theta)^2} \right] - \omega_{ij} q_{ij}^*. \end{aligned} \quad (33)$$

And q_{ij}^{k+1} can be obtained similarly for each i row. The finite difference format is the same as that in Ref. [5].

3. Results and discussions

3.1. The density distributions of three structures

As we know, the geometrical confinement effects of polymer chains can be studied by investigating their configurations. Just by the distributions of these configurations do we know the properties of polymer solutions. These studies are also helpful for us when we deal with the industrial and other applications. In the followings, we will discuss the density distributions of loop, tail and bridge.

Fig. 1 shows the loop distributions. The loop structure distributions, which being about the range of $1 \sim 2b$, around the surfaces of the particles symmetrically, and decreases gradually to zero far away from the surface. When $d = 10$, the loops distribute mainly around the surfaces of the two spheres. These behaviors are similar to the result of the case of one sphere, which is in Fig. 2 of Ref. [4]. But if we take $d = 4$, namely decreasing the distance of the two spheres, we can see the loop distribution near the surface of spheres decreases greatly. This is a result of spatial confinement, since the chains must gain more entropy. Obviously, this phenomenon of the bispherical system does not presented in the case of one sphere. By the way, this plot includes the configurations that the same polymer is adsorbed asymmetrically to the two colloidal particles. In one case, more polymers are adsorbed on one particle which denoted by particle 1 than another by particle 2. However, there is another case that more polymers are adsorbed on particle 2 than particle 1. And the probability is the same for these two cases. The distributions of Fig. 1 are the mean results in our paper.

Fig. 2 is the distributions of the tail structures. Comparing to the loop structure, the tail distribution dominates in a larger region away from the particle surface. Like the loop structure, as the separation between the two particles is diminishing, from $d = 10$ to $d = 4$, the tail structure in the middle region decreases. It also arises from the spatial confinement. Thus we can conclude that in the domain nearby the surface of the sphere, there is mainly loop distribution. In a larger region, tail distribution dominates. While in a further region, it is mostly free chain distributions. Thus we can conclude that the tail plays an important role in determining the properties of the polymer-colloid mixtures. The bispherical coordinate calculation can tell us new phenomenon which we cannot find in the sphere-symmetrical coordinate [4].

Fig. 3 shows the distributions of the bridge structure. We can find that the bridge structure mainly distributes around the middle region of the two spheres. When one particle is approaching to another, or, from $d = 10$ to $d = 4$, the density profile increases greatly, from about 0.02 to 0.4, which has a magnitude order in difference. Obviously, it cannot be ignored and this is a new phenomenon. From this new phenomenon we can find that the bridge structure plays an important role in determining the

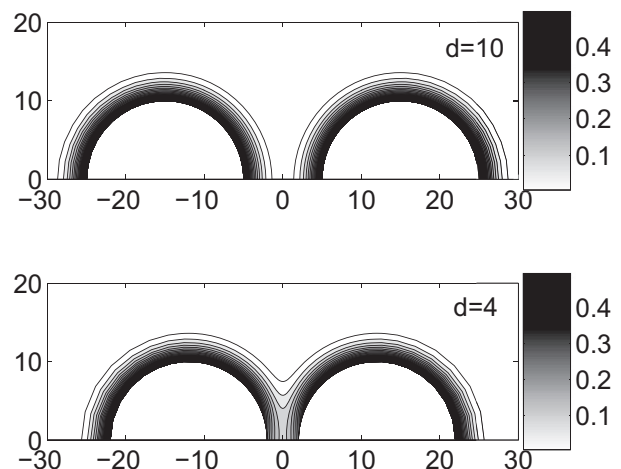


Fig. 1. Contour plots of the loop distributions for $d = 10$ (d , in the unit of the statistical segment length b , is the separation between the two particles) and $d = 4$, respectively. The horizontal axis is the line which connects with two centers of the particles. The distribution values of the button bars are in unit of the polymer bulk concentration. The other parameters are the same for both cases: $R = 10$, $\phi^0 = 0.1$, $\chi = 0.5$, $\kappa = 0.5$, $N = 100$ and $R_g \sim 4.1$.

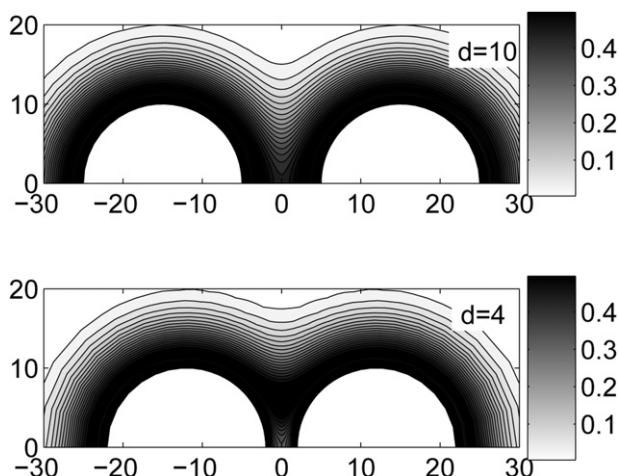


Fig. 2. Contour plots of the tail distributions for $d = 10$ and $d = 4$, respectively. The other parameters are the same as Fig. 1.

properties of the polymer-colloid mixtures. As we know that when adding nanoparticles into the polymer solutions or polymer melts, the tails will entangle each other. The bridge will contribute to the entanglement as we can see from its definition. Thus the bridge structure affect the excess entanglements of the polymer solution in addition tail structure. In the case of one sphere [4], the authors did not discuss the bridge structure, since there is no bridge structure for one sphere.

Likewise, the surface curvature of particle is an important ingredient in the study of structures. By the similar analysis as the above, we can also draw the conclusion that the bridge structures play important effects when changing the radius of the nanoparticle.

3.2. Potential between the two spheres

The potential is a key physical quantity which dominates the property of the colloid-polymer mixtures. Since the polymer chains have some configurations, and every different configuration contributes differently to the potential. Both loop and tail contribute repulsive potentials. However, free and bridge structures contribute adsorptive potentials as they decrease the configuration entropy. So whether or not certain configuration arising maybe

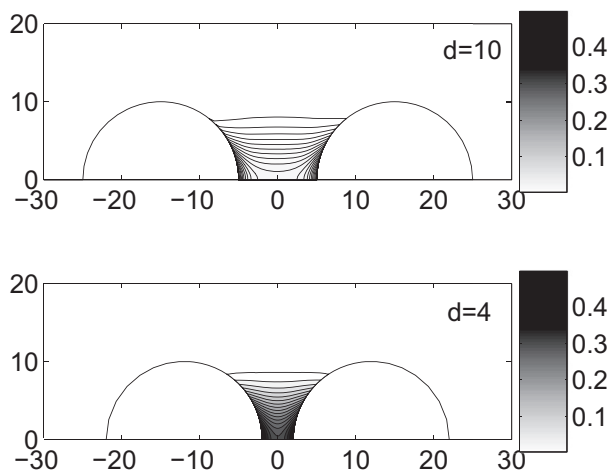


Fig. 3. Contour plots of the bridge distributions for $d = 10$ and $d = 4$, respectively. The other parameters are the same as Fig. 1.

affect the potential greatly. There are many quantitative studies about the contributions to the potential of different configurations, such as, the study of polymer-grafted system by Matsen, depletion potential between two colloidal particles in non-adsorbing polymer solutions in Ref. [5]. In these studies, the free and adsorbed propagators are well defined. Therefore the definitions of many physical quantities, for example, contribution to the potential of each configuration become quite clear. Especially, the tail fraction and the loop fraction can be well defined in the case of one sphere in Ref. [4], thus they can give individual contribution of each structure to the potential. In this subsection we will investigate the potential between two spheres.

Fig. 4 shows the potential U between the two spheres as a function of the separation d under the polymer bulk concentrations $\phi^0 = 0.01, 0.02, 0.04, 0.06$, when the other parameters are taken as $\kappa = 0.1, R = 10, \chi = 0.5$ and $N = 100$. From $\phi^0 = 0.01, 0.02$ and 0.04 , we find that the potential depth increases with increasing polymer concentration. When the distance of the two nanoparticles are greater than 10, the potential nearly vanishes, once the distance is smaller than 10, then the potential will change. But the change of U is very small, it is about -0.05 . Obviously this is an attractive potential.

We know that the tails which absorbed on two different nanoparticles repel each other, and this will contribute an effective repulsive potential if we diminish the spacing of the two nanoparticles. Also do the loops, though they distribute mainly around the surface of the nanoparticle. However, the contributions of the bridge configurations are different. The bridge connects with two nanoparticles, according to classical physics, this configuration will give an effective adsorptive potential to the system. The potential is the total effect of the effective adsorptive potential and the effective repulsive ones, and the two effective potentials compete with each other.

Therefore, we can interpret the results of Fig. 4 as follows. When the spacing of two nanoparticles diminishes, the concentration of the tail structure will decrease. On the contrary, the concentration of the bridge structure will increase, and the total effect of these two ones makes the potential curve very flat. When increasing the polymer concentration, more polymer chains have chance to form bridge. Therefore, when two nanoparticles approaching, the higher the concentration is, the deeper the potential depth is.

In the present case, the interaction is always attractive. This is different from that in Ref. [12], which is always repulsive. Because in Ref. [12], the number of the polymer chains on the surface is fixed, which represents a repulsive interaction. While in the present case, the number of the polymer chains is changeable. When the separation is very small, the number of the polymer

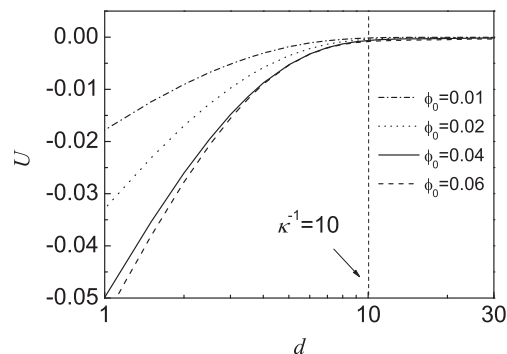


Fig. 4. Relations of the potential U between the two spheres and the separation d (in unit of b) in dilute solutions with the polymer bulk concentrations $\phi^0 = 0.01, 0.02, 0.04, 0.06$, respectively, when $\kappa = 0.1$. The other parameters are $R = 10, \chi = 0.5, N = 100$.

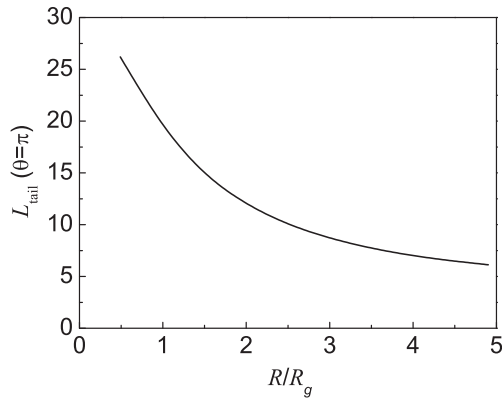


Fig. 5. The average tail length $L_{\text{tail}}(\theta)$ (in unit of Kuhn length b) when $\theta = \pi$ as the function of particle radius (normalized by R_g) under $\phi^0 = 0.1$. The other parameters are taken as $\chi = 0.5$, $d = 4$, $N = 100$, $R_g = 4.1$, $\kappa = 0.5$.

chains diminishes, and at the same time, the bridging increases, the adsorption could not resist the spatial confinement. Thus, an attractive interaction dominates now.

3.3. The average tail length

Entanglements of polymer chains are very important in studying polymer solutions. Generally speaking, the most important physical quantity is the average tail length in the study of entanglements of polymer solutions [4]. However, in addition the tail structure, the bridge structure has an important contribution to the entanglement effect in the present case. In this subsection, we would like to consider the average tail length $L_{\text{tail}}(\theta)$ when $\theta = \pi$, for $L_{\text{tail}}(\pi)$ changes considerably and can reflect the behavior of bispherical system well.

Fig. 5 shows $L_{\text{tail}}(\pi)$ as functions of sphere radius R (normalized by R_g) when bulk concentrations is taken 0.1. We find that the average tail length is a decreasing function of the sphere radius, which is similar to that in Ref. [4]. As the sphere becomes larger, $L_{\text{tail}}(\pi)$ becomes smaller. When the spheres become very large, they can be considered as two plates. As a result of entropy penalty, there are few polymer coils in the gap, and this leads $L_{\text{tail}}(\pi)$ to become very small.

Fig. 6 shows how $L_{\text{tail}}(\pi)$ varies with separation d of two nanoparticles under $\phi^0 = 0.1$. In this diagram, one can find that $L_{\text{tail}}(\pi)$ increase as separation d increasing. When the separation is a few R_g , the curves become quite flat. This is because when one sphere is away from another, the effect of confinement diminishes, and

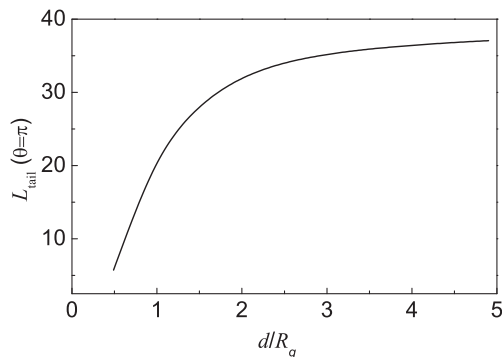


Fig. 6. The average tail length $L_{\text{tail}}(\theta = \pi)$ (in unit of b) as the function of d (normalized by R_g) under $\phi^0 = 0.1$. The other parameters are taken as $\chi = 0.5$, $R = 4$, $N = 100$, $\kappa = 0.5$.

the polymer chain can stay more and more freely in the gap. The average length of the tails does not increase any more.

4. Conclusions

In this paper, we employ the SCFT to study the density distributions of the loop, tail and bridge in an adsorptive polymer solution under the bispherical coordinates. We find that the bridge structure has an important contribution in the present case. In addition, we also discuss the separation dependent potential between two colloidal particles. The results show that the interaction is always attractive, whose depth is smaller than that of the pure depletion interaction. Finally, we find that the average tail length decrease as the radius of the colloidal particle increase, but the average tail length increases as two colloidal particles are awaying from each other.

Acknowledgments

The authors would like to acknowledge helpful discussions with Dr. Tongchuan Suo and Dr. Shuang Yang. This work is supported by the National Natural Science Foundation of China (NSFC) Nos. 2090234, 20973176, 973 Program of the Ministry of Science and Technology (MOST) 2011CB808502, and the Fundamental Research Funds for the Central University.

Appendix

The boundary condition $\nabla q(\mathbf{r}, t) \cdot \hat{\mathbf{n}} + \kappa q(\mathbf{r}, t) = 0$ can be reformulated in bispherical coordinates, where the unit vector $\hat{\mathbf{n}}$ is the exterior normal vector of the spherical surface, while κ is the parameter which characterizes the adsorptive interaction. The infinitesimal line element in Cartesian coordinates (x, y, z) is given by

$$ds^2 = dx^2 + dy^2 + dz^2, \quad (34)$$

while in a general curvilinear coordinate system (ξ_1, ξ_2, ξ_3) it is,

$$ds^2 = \sum_{i=1,2,3} h_i^2 d\xi_i^2, \quad (35)$$

and,

$$h_i^2 = \left(\frac{\partial x}{\partial \xi_i} \right)^2 + \left(\frac{\partial y}{\partial \xi_i} \right)^2 + \left(\frac{\partial z}{\partial \xi_i} \right)^2, \quad (36)$$

where h_i , $i = 1, 2, 3$, is called the scalar factor of coordinate system (ξ_1, ξ_2, ξ_3) , in particular, $i = \eta, \theta, \varphi$ for bispherical coordinates.

Let $(\mathbf{i}, \mathbf{j}, \mathbf{k})$ and $(\mathbf{e}_\eta, \mathbf{e}_\theta, \mathbf{e}_\varphi)$ are the unit vectors for Cartesian coordinate and the general curvilinear coordinate system respectively. For a scalar function q , its gradient can be written as follows,

$$\nabla q = \frac{\partial q}{\partial x} \mathbf{i} + \frac{\partial q}{\partial y} \mathbf{j} + \frac{\partial q}{\partial z} \mathbf{k}, = \frac{1}{h_\eta} \frac{\partial q}{\partial \eta} \mathbf{e}_\eta + \frac{1}{h_\theta} \frac{\partial q}{\partial \theta} \mathbf{e}_\theta + \frac{1}{h_\varphi} \frac{\partial q}{\partial \varphi} \mathbf{e}_\varphi. \quad (37)$$

By the relations between bispherical coordinates (η, θ, φ) and Cartesian coordinates (x, y, z) , we can obtain,

$$\mathbf{e}_\eta = \frac{\frac{\partial x}{\partial \eta} \mathbf{i} + \frac{\partial y}{\partial \eta} \mathbf{j} + \frac{\partial z}{\partial \eta} \mathbf{k}}{\sqrt{\left(\frac{\partial x}{\partial \eta} \right)^2 + \left(\frac{\partial y}{\partial \eta} \right)^2 + \left(\frac{\partial z}{\partial \eta} \right)^2}}, \quad (38)$$

$$\frac{\partial x}{\partial \eta} = \frac{a \sin \theta \cos \varphi \sinh \eta}{(\cosh \eta - \cos \theta)^2}, \quad \frac{\partial y}{\partial \eta} = \frac{a \sin \theta \sin \varphi \sinh \eta}{(\cosh \eta - \cos \theta)^2},$$

$$\frac{\partial z}{\partial \eta} = \frac{a(1 - \cos \theta \cosh \eta)}{(\cosh \eta - \cos \theta)^2}, \quad (39)$$

$$h_\eta = \sqrt{\left(\frac{\partial x}{\partial \eta}\right)^2 + \left(\frac{\partial y}{\partial \eta}\right)^2 + \left(\frac{\partial z}{\partial \eta}\right)^2} = \frac{a}{\cosh \eta - \cos \theta}, \quad (40)$$

for η ; and,

$$\mathbf{e}_\theta = \frac{\frac{\partial x}{\partial \theta} \mathbf{i} + \frac{\partial y}{\partial \theta} \mathbf{j} + \frac{\partial z}{\partial \theta} \mathbf{k}}{\sqrt{\left(\frac{\partial x}{\partial \theta}\right)^2 + \left(\frac{\partial y}{\partial \theta}\right)^2 + \left(\frac{\partial z}{\partial \theta}\right)^2}}, \quad (41)$$

$$\frac{\partial x}{\partial \theta} = \frac{a \cos \varphi (\cos \theta \cosh \eta - 1)}{(\cosh \eta - \cos \theta)^2}, \quad \frac{\partial y}{\partial \theta} = \frac{a \sin \varphi (\cos \theta \cosh \eta - 1)}{(\cosh \eta - \cos \theta)^2},$$

$$\frac{\partial z}{\partial \theta} = \frac{a \sin \theta \sinh \theta}{(\cosh \eta - \cos \theta)^2}, \quad (42)$$

$$h_\theta = \sqrt{\left(\frac{\partial x}{\partial \theta}\right)^2 + \left(\frac{\partial y}{\partial \theta}\right)^2 + \left(\frac{\partial z}{\partial \theta}\right)^2} = \frac{a}{\cosh \eta - \cos \theta}, \quad (43)$$

for θ ; and,

$$\mathbf{e}_\varphi = \frac{\frac{\partial x}{\partial \varphi} \mathbf{i} + \frac{\partial y}{\partial \varphi} \mathbf{j} + \frac{\partial z}{\partial \varphi} \mathbf{k}}{\sqrt{\left(\frac{\partial x}{\partial \varphi}\right)^2 + \left(\frac{\partial y}{\partial \varphi}\right)^2 + \left(\frac{\partial z}{\partial \varphi}\right)^2}}, \quad (44)$$

$$\frac{\partial x}{\partial \varphi} = \frac{a \sin \theta \sin \varphi}{\cosh \eta - \cos \theta}, \quad \frac{\partial y}{\partial \varphi} = \frac{a \sin \theta \cos \varphi}{\cosh \eta - \cos \theta}, \quad \frac{\partial z}{\partial \varphi} = 0, \quad (45)$$

$$h_\varphi = \sqrt{\left(\frac{\partial x}{\partial \varphi}\right)^2 + \left(\frac{\partial y}{\partial \varphi}\right)^2 + \left(\frac{\partial z}{\partial \varphi}\right)^2}, \quad (46)$$

for φ . Surface $\eta = \eta_0$ is a sphere $x^2 + y^2 + (z - a \coth \eta_0)^2 = (a/\sinh \eta_0)^2$ [19], and its exterior normal unit vector is given by,

$$\hat{\mathbf{n}} = \frac{(x, y, z - a \coth \eta)}{|a/\sinh \eta|}. \quad (47)$$

Then we can obtain,

$$-\frac{\cosh \eta - \cos \theta}{\sinh \eta} \frac{\partial}{\partial \eta} q + \left| \frac{a}{\sinh \eta} \right| \kappa q = 0. \quad (48)$$

For surface η_+ , $\sinh \eta_+ > 0$, the boundary condition is given by,

$$\frac{\partial}{\partial \eta} q - \frac{a\kappa}{\cosh \eta - \cos \theta} q = 0, \quad (49)$$

while for surface η_- , $\sinh \eta_- < 0$, and the boundary condition is given by,

$$\frac{\partial}{\partial \eta} q + \frac{a\kappa}{\cosh \eta - \cos \theta} q = 0. \quad (50)$$

References

- [1] Jaworski S, Sikorski A. *Polymer* 2012;53:1741.
- [2] Urza MD, Briones XG, Carrasco LP, Encinas MV, Petri DFS. *Polymer* 2010;51:3445.
- [3] FLeer GJ, Cohen Stuart M, Schjeutjens JMHJ, Cosgrove T, Vincent B. *Polymer in interface*. London: Chapman & Hall; 1993.
- [4] Yang S, Yan DD, Shi AC. *Macromolecules* 2006;39:4168.
- [5] Yang S, Yan DD, Tan HG, Shi AC. *Phys Rev E* 2006;74:041808.
- [6] Asakura S, Oosawa F. *J Chem Phys* 1954;22:1255.
- [7] de Gennes PG. *Scaling concepts in polymer physics*. Ithaca and London: Cornell University Press; 1979.
- [8] Feigin RI, Napper DH. *J Colloid Interface Sci* 1980;75:525.
- [9] Joanny JF, Leibler L, de Gennes PG. *J Polym Sci Polym Phys Ed* 1979;17:1073.
- [10] Scheutjens JHMH, FLeer GJ. *Adv Colloid Interface Sci* 1982;16:361.
- [11] Aubouy M, Raphael E. *Macromolecules* 1998;31:4357.
- [12] Kim JU, Matsen MW. *Macromolecules* 2008;41:4435.
- [13] Kim Y, Park CB, Chen P, Thompson RB. *Polymer* 2011;52:5622.
- [14] Kim SH, Cochran EW. *Polymer* 2011;52:2328.
- [15] Suo TC, Yan DD. *Polymer* 2011;52:1686.
- [16] Matsen MW. *J Chem Phys* 1995;102:3884.
- [17] Morse PM, Feshbach H. *Methods of theoretical physics*. New York: McGraw-Hill; 1990.
- [18] Cook GB. *Phys Rev D* 1991;44:2983.
- [19] Roan JR, Kawakatsu T. *J Chem Phys* 2002;116:7283.
- [20] Hong KM, Noolandi J. *Macromolecules* 1981;14:727.
- [21] Wood SM, Wang ZG. *J Chem Phys* 2002;116:2289.
- [22] Ames WF. *Numerical methods for partial differential equation*. Boston: Academic; 1992.